JOURNAL OF GUIDANCE, CONTROL, AND DYNAMICS
Vol. 34, No. 2, March–April 2011

Optimal Rotation Sequences in Presence of Constraints on Admissible Rotation Axes

Giulio Avanzini* and Luca Berardo†
Politecnico di Torino, 10129 Turin, Italy
Fabrizio Giulietti‡
University of Bologna, 47100 Forlì, Italy
and
Edmondo A. Minisci§
University of Glasgow, Glasgow, Scotland G12 8QQ, U.K.

DOI: 10.2514/1.49805

In underactuated conditions, satellite attitude actuators can deliver a control torque with two components only. The paper develops a general solution for the problem of attitude maneuver planning for underactuated spacecraft by means of a sequence of N admissible rotations, where a rotation is considered to be admissible if it takes place around an axis which lies on the plane where the actuator system can deliver a control torque. An exact solution for the sequence of two feasible rotations that provides a desired reorientation is derived, where the minimum angular-path sequence can also be identified analytically. The optimal sequence for a higher number of steps is obtained by means of a numerical optimization procedure. The features of the optimal sequences for increasing values of N are investigated in order to obtain a better understanding of their characteristics.

Nomenclature

$\hat{\boldsymbol{a}}$	=	Euler eigenaxis associated to a generic rotation $\mathcal{Q}$
$\hat{\boldsymbol{b}}$	=	torqueless direction
$\boldsymbol{E}$	=	quaternion error vector
$\hat{\boldsymbol{e}}$	=	nominal Euler axis
$\mathcal{F}_{(\cdot)}$	=	reference frame
N	=	number of admissible rotations in a sequence
$\boldsymbol{Q}$	=	quaternion associated to a generic rotation $\mathcal{Q}$, $[\boldsymbol{q}^T, \bar{q}]^T$
$\hat{\boldsymbol{g}}$	=	nonnominal Euler axis
$\boldsymbol{q}$	=	vector part of quaternion $\boldsymbol{Q}$, $\hat{\boldsymbol{a}}\sin(\alpha/2)$
$\bar{q}$	=	scalar part of quaternion $\boldsymbol{Q}$, $\cos(\alpha/2)$
$\mathcal{Q}(\hat{\boldsymbol{a}}, \alpha)$	=	rotation of α around $\hat{\boldsymbol{a}}$, associated to the quaternion $\boldsymbol{Q}$
$\mathbb{T}_{BA}$	=	coordinate transformation matrix from frame $\mathcal{F}_A$ to $\mathcal{F}_B$
α	=	Euler eigenaxis rotation amplitude associated to a generic rotation $\mathcal{Q}$
$\hat{\alpha}_i$	=	angular position of ith admissible nonnominal eigenaxes on Γ, deg
Γ	=	plane of admissible rotation axes
λ	=	angle between nominal Euler eigenaxis and torqueless direction, $\cos^{-1}(\hat{\boldsymbol{e}} \cdot \hat{\boldsymbol{b}})$, deg
ε	=	misalignment error, deg
ϵ	=	scalar part of the quaternion error vector $\boldsymbol{E}$, $\cos(\varepsilon/2)$
ϕ	=	nominal Euler rotation angle around $\hat{\boldsymbol{e}}$, deg
$\hat{\phi}_i$	=	rotation angle around ith admissible nonnominal eigenaxes $\hat{\boldsymbol{g}}_i$, deg

Subscripts

B	=	body frame
BO	=	fixed to body frame rotation
C	=	generic final attitude after two rotations
O	=	fixed frame
T	=	target frame
1	=	first rotation
2	=	second rotation

Superscripts

T	=	transpose
$*$	=	conjugate

Introduction

THIS paper develops a general solution for the problem of attitude maneuver planning by means of a sequence of admissible rotations for spacecraft operating in underactuated conditions, when attitude effectors can deliver a control torque with two components only for controlling three rotational degrees of freedom. The problem of controlling underactuated spacecraft has recently gained great interest among researchers, where the spacecraft can become underactuated because of a failure in a minimal control system, multiple failures in a redundant one and/or physical characteristics of the attitude control hardware, as for magnetic actuators, the latter being an attractive option for low-Earth-orbit small satellites thanks to its reduced mass, power consumption, and system complexity when compared with wheel based actuators or gas jet thrusters [1].

Control of underactuated systems received considerable attention in the robotic literature. Many examples rely on the application of a geometric nonlinear control framework to mechanical systems in general, and underactuated ones in particular [2], but, to the authors' knowledge, no general solution to the problem of underactuated satellite attitude control has yet been found, in spite of a considerable amount of work on the subject. It is worth remembering that if only two independent torque components are available for controlling three attitude degrees of freedom, the problem of attitude regulation

Received 9 March 2010; revision received 20 September 2010; accepted for publication 8 November 2010.

*Assistant Professor, Department of Aerospace Engineering, C.so Duca degli Abruzzi 24; giulio.avanzini@polito.it. Senior Member AIAA (Corresponding Author).

†Graduate Student, Department of Aerospace Engineering, C.so Duca degli Abruzzi 24.

‡Assistant Professor, Department of Mechanical and Aerospace Engineering, Via Fontanelle 40. Senior Member AIAA.

§Research Fellow, Department of Aerospace Engineering, James Watt South Building.

is not solvable by means of continuous (static or dynamic) time-invariant control laws, as stated in Byrnes and Isidori [3].

The techniques considered in the literature for solving this challenging control problem range from relatively simple kinematic approaches for damping out the angular velocity vector by use of external control torques, such as gas jets or magnetotorquers [4–8] to more complex scenarios, where stabilization of a prescribed attitude is pursued [3,9–14]. When spacecraft attitude control is obtained by use of internal torques generated by momentum exchange devices, gyroscopic coupling makes the issue of underactuated attitude control even more difficult [15–20].

Attitude control systems based on magnetic-torque only make the satellite inherently underactuated, as internal magnetic coils can generate torques in a direction perpendicular to the magnetic field vector [21]. In many applications a momentum wheel is added to the system in order to gyroscopically stabilize the spacecraft and to obtain a nominal control problem, where attitude effectors can deliver arbitrary control torque in space, within their saturation limits. Nonetheless, a considerable amount of work has been dedicated to the problems of analysis and design of purely magnetic control laws, as a safe control mode, in case of wheel failure, or even as the nominal control mode, for purely magnetic configurations [1,22–25]. As a matter of fact, the system remains controllable if the orbit has an adequate inclination, as the Earth's magnetic field vector rotates in space while the satellite moves around its orbit. This makes the satellite an approximately periodically time-varying system. This latter fact, together with the system underactuation, originates a challenging control design problem.

The solutions proposed so far are thus strongly related to the type of control hardware considered and applicative scenarios. A computationally efficient maneuver planning scheme that provides a general solution for the definition of a (sequence of) feasible rotation (s) that can drive an underactuated satellite towards a desired target attitude is thus an interesting option, as a first step in the determination of a maneuver strategy. This paper thus aims at providing a general purely kinematic solution to the problem of underactuated satellite maneuver planning.

In this framework, a rotation described by means of the direction of its rotation axis $\hat{\boldsymbol{g}}$ and amplitude $\hat{\phi}$ is defined as admissible if $\hat{\boldsymbol{g}}$ lies on the plane where attitude effectors can actually deliver a control torque, that is, any direction perpendicular to the axis $\hat{\boldsymbol{b}}$ around which the control hardware cannot deliver a torque component. The definition of a sequence of N admissible rotations that drives the spacecraft onto (or at least sufficiently close to) a prescribed desired attitude can provide a method for planning attitude maneuvers in the framework of a failure-mode of operations for minimal attitude control systems, if the sequence of attitude slews can still be tracked with a sufficient level of accuracy. On the other hand, the proposed technique may represent a planning scheme for feasible attitude maneuvers of magnetic controlled spacecraft, which are inherently underactuated.

A dynamic implementation of the maneuver thus determined quite obviously requires the identification of a suitable control action, such that the final pointing error remains sufficiently small in order to perform (at least part of) mission operations in spite of a possible actuator failure. Such an analysis should be based on a dynamic model which includes at least Euler's rigid body equations, when not also the effects of flexible modes for large space structures or in the presence of flexible appendages [26]. Nonetheless, the definition of a general maneuver planning technique, totally independent of the particular spacecraft configuration or equipment, represents in itself an interesting result.

The problem of planning attitude maneuvers for underactuated spacecraft by means of a kinematic approach was first addressed by Giulietti and Tortora [27], who analytically determined the nonnominal rotation axis $\hat{\boldsymbol{g}}$ and the relative rotation angle, $\hat{\phi}$, that allow for minimizing the angular error from a prescribed target attitude represented by means of a nominal Euler eigenaxis rotation ϕ about the eigenaxis $\hat{\boldsymbol{e}}$. They showed that the resulting misalignment error, ε, after the best feasible rotation grows with the dot product $\hat{\boldsymbol{e}} \cdot \hat{\boldsymbol{g}}$. More recently, Avanzini and Giulietti [28] demonstrated that it is always possible to determine a single admissible eigenaxis rotation that makes a single body-fixed axis parallel to a prescribed direction in space: rather than trying to minimize the overall misalignment with respect to a given attitude, which may result in a pointing error too large for any practical purposes, the pointing of a single sensor or hardware element along a prescribed direction is tracked as accurately as possible.

These previous studies provided the two best options available with a single feasible eigenaxis rotation, either the minimum overall misalignment error or exact pointing of a single body-fixed axis. The present study aims at generalizing the problem of kinematic planning of feasible maneuvers in the presence of constraints on the direction of admissible rotation axes to sequences of N admissible rotations. An analytical solutions for $N = 2$ is derived, showing the following:

1) Two rotations are always sufficient for reaching any target attitude from the initial one.

2) The optimal, minimum angular travel sequence can be determined analytically, leading to a small computational effort.

Although in the general case of a three-inertial satellite the minimum angular travel does not result into a minimum energy solution or a fuel optimal one, the three solutions coincide for a satellite with equal principal moments of inertia, and differences are rather mild when inertias around the principal axes are of the same order of magnitude. This means that a minimum angular travel provides a suboptimal solution, if energy cost is considered as the performance index, but the increase in energy expenditure is marginal for small cube-sats, with a quasi-spherical inertia tensor. The availability of an analytical solution for the minimum angular path makes the kinematic maneuver planning technique particularly interesting for small, low-cost spacecraft, where operational requirements may not be extreme, while computational power available is limited and cost and weight penalties associated with redundancy may result unacceptable. In this respect, the interest for simple, numerically efficient maneuver planning schemes becomes evident when one considers the ever increasing demand over the last years for small satellites, due to their cheaper cost, milder requirements on launcher capabilities, and potential for high operational performance when appropriately coordinated in formations or constellations [29].

A general solution for $N > 2$ is then developed by means of a numerical optimization technique, which allows for determining minimum angular path sequences of admissible rotations for achieving any desired attitude. It should be noted that, given the analytical solution for the $N = 2$ rotation sequence, it is possible to derive an unconstrained formulation for the optimization problem of the $N > 2$ case. Every rotation features two parameters (one for the direction of the rotation axis on the plane of admissible axes, and the amplitude of the corresponding rotation), so that the total number of unknowns is, in general, $2N$, with three constraints on the components of the final quaternion error [26] that must be zero in order to achieve the prescribed final attitude. For $N = 2$, three of the parameters (namely the amplitude of the first rotation, the position of the second rotation axis and the corresponding rotation angle) are determined analytically as a function of the position of the first axis, so that the resulting optimization problem depends on one variable only, which allows for a closed form solution. When $N > 2$ rotations are considered, it is possible to divide the sequence into two parts: an initial sequence of $N - 2$ rotations that takes the spacecraft onto an intermediate attitude, and a final sequence of two rotations determined according to the analytical solution that achieves the prescribed target attitude, starting from the intermediate one. The total number of optimization variables is thus $2(N - 2) + 1$ and the constraint on the final attitude is enforced by the last two steps of the maneuver.

A sequential-quadratic programming (SQP) algorithm is used for solving the resulting unconstrained minimization problem. Unfortunately, the sequence of rotations presents several local minima for the total angular displacement, so that a multistart (MS) algorithm was used in order to identify the best possible sequence by spanning the search space as accurately as possible. The so-called monotonic basin hopping (MBH) algorithm was adopted, an optimization

method based on multiple local searches with a gradient method. The MBH technique, developed by Wales and Doye for tackling a specific global optimization problem for molecular conformations [30], is particularly well suited for optimization problems featuring a funnel functional shape [31], but more recently it was brought to a mature state where it can efficiently solve generic global optimization problems [32,33].

In its basic version it is quite similar to a generic MS method, which is also based on multiple local searches, the major yet decisive difference being represented by the distribution of the initial guesses: the MS approach randomly generates the starting points of the optimization process over the whole search space, while the MBH algorithm generates them in a neighborhood $\mathcal{N}_\rho(\boldsymbol{x})$ of the current local minimum $\boldsymbol{x}$. The correct choice of the parameter ρ that determines the size of the neighborhood is essential for performance. A small value causes the generation of random points within the basin of attraction of the current local minimum only, thus harming the convergence to the global minimum, but if ρ is too large, the MBH algorithm behaves substantially like the standard MS method. A careful choice of ρ may lead to results which strongly outperform those of the simpler MS approach, in spite of the apparently mild difference between the two algorithms.

As stated before, the MBH is particularly well suited for problems with a funnel-like structure for the function to be minimized, but for more complex functional shapes featuring a multiple-funnel structure, the effectiveness of the MBH should be improved with a global resampling [34], that is, when the value of the estimate of the global solution does not change for a certain number of iterations, the search restarts from a point randomly sampled in the whole search space. This latter method was employed in the present work, because of the unknown size of the basins of attractions for the local optima and the resultant uncertainty on a correct choice for ρ. Thanks to the capability of the MBH approach to jump from one basin of attraction to a neighboring one, it was possible to efficiently identify optimal sequences of rotations for N as large as 12, in spite of the presence of a rather complex structure of local minima in the $(2N-3)$-dimensional search space.

The most interesting result obtained from the analysis of the minimum angular travel solutions is that every optimal sequence always features rotations of equal amplitude with eigenaxes that are symmetrically placed with respect to the projection of the nominal eigenaxis on the plane of admissible rotations.

In the sequel, a brief section of preliminaries on the use of quaternions is presented, in order to introduce the notation used in the paper. The analytical solution for a sequence of two rotations is then derived in the following section and the properties of the sequence analyzed. Then, the problem of minimum angular displacement for a generic sequence of N rotations is stated and numerically solved by means of the multistart algorithm for global minimization. A Section of Conclusions ends the paper.

Notation and Mathematical Preliminaries

The problem of optimal rotation sequences will be stated by making use of the quaternions for describing both attitudes with respect to a prescribed fixed frame $\mathcal{F}_O$ and rotations $\mathcal{R}$. This section, rather than a review of well known concepts that can be found in several textbooks (e.g. [21,26] and many others), is included in order to introduce the notation adopted in the sequel, while highlighting the strict relation between eigenaxis rotations and quaternions, which is at the basis of the present work. In this framework, the results taken from [27] will be recast in quaternion formulation, so that, together with a generalization to the case of optimal sequences of $N > 1$ rotations, a uniform notation is adopted for all the considered cases.

The attitude of a body frame $\mathcal{F}_B$ with respect to a fixed reference frame $\mathcal{F}_O$ can be described by means of the quaternion vector $\boldsymbol{Q}$, defined as

$$\boldsymbol{Q} = [\boldsymbol{q}^T, \bar{q}]^T \qquad = [\hat{\boldsymbol{a}}^T \sin(\alpha/2), \cos(\alpha/2)]^T$$

where α is the amplitude of the so-called Euler eigenaxis rotation that takes $\mathcal{F}_O$ onto $\mathcal{F}_B$, the unit vector $\hat{\boldsymbol{a}}$ representing the eigenaxis. The rotation associated with the quaternion $\boldsymbol{Q}$ is indicated as $\mathcal{Q}(\hat{\boldsymbol{a}}, \alpha)$. Note that the inverse rotation that takes $\mathcal{F}_B$ onto $\mathcal{F}_O$ is described by the conjugate quaternion $\boldsymbol{Q}^* = [-\boldsymbol{q}^T, \bar{q}]^T = [-\hat{\boldsymbol{a}}^T \sin(\alpha/2), \cos(\alpha/2)]^T$, which represents a rotation with the same amplitude around the same axis, but in the opposite direction, $\mathcal{Q}^* = \mathcal{Q}(\hat{\boldsymbol{a}}, -\phi)$, or an equivalent angular displacement around an axis oriented in the opposite direction, $\mathcal{Q}^* = \mathcal{Q}(-\hat{\boldsymbol{a}}, \phi)$.

Given two quaternions $\boldsymbol{Q} = [\boldsymbol{q}^T, \bar{q}]^T = [\hat{\boldsymbol{a}}^T \sin(\alpha/2), \cos(\alpha/2)]^T$ and $\boldsymbol{R} = [\boldsymbol{r}^T, \bar{r}]^T = [\hat{\boldsymbol{b}}^T \sin(\beta/2), \cos(\beta/2)]^T$, the quaternion multiplication operation [26]

$$\boldsymbol{S} = [\boldsymbol{s}^T, \bar{s}]^T = \boldsymbol{Q}\boldsymbol{R}$$

is defined as

$$\begin{aligned} \boldsymbol{s} &= \bar{q}\boldsymbol{r} + \bar{r}\boldsymbol{q} + \boldsymbol{q} \times \boldsymbol{r} = \hat{\boldsymbol{g}} \sin(\gamma/2); \\ \bar{s} &= \bar{q}\,\bar{r} - \boldsymbol{q} \cdot \boldsymbol{r} = \cos(\gamma/2) \end{aligned} \tag{1}$$

The resulting quaternion $\boldsymbol{S}$ represents the final attitude of a frame $\mathcal{F}_C$ obtained from $\mathcal{F}_O$ by means of a sequence of two rotations $\mathcal{Q}(\hat{\boldsymbol{a}}, \alpha)$ and $\mathcal{R}(\hat{\boldsymbol{b}}, \beta)$, described by $\boldsymbol{Q}$ and $\boldsymbol{R}$ respectively (where $\hat{\boldsymbol{b}}$ is represented in the intermediate frame $\mathcal{F}_B$). The quaternion $\boldsymbol{S}$ provides the information on the single rotation $\mathcal{S}(\hat{\boldsymbol{g}}, \gamma)$, that takes $\mathcal{F}_O$ directly onto $\mathcal{F}_C$.

It is easy to show that the quaternion multiplication is associative but it is not commutative. The quaternion multiplication can thus be used for determining the final attitude after a sequence of rotations, each one described by means of the corresponding axis and rotation angle. At the same time, the quaternion multiplication operation allows also for the definition of the quaternion error vector [26], which in turn provides a direct measure of the misalignment error, with a simple set of operations.

In this latter framework, letting $\mathcal{F}_T$ be the desired (target) position, described by means of the quaternion $\boldsymbol{P}$, the amplitude ε of the eigenaxis rotation $\mathcal{E}$ from $\mathcal{F}_T$ to $\mathcal{F}_B$ represents the misalignment error of the current attitude, that is, the amplitude of the rotation that one should perform to align the present attitude with the desired one (Fig. 1a). The corresponding quaternion $\boldsymbol{E} = [\boldsymbol{\epsilon}^T, \bar{\epsilon}]^T$ that satisfies the equation $\boldsymbol{P}\boldsymbol{E} = \boldsymbol{Q}$ is the quaternion error

$$\boldsymbol{E} = \boldsymbol{P}^*\boldsymbol{Q}$$

Note that when a time-invariant target frame is considered, it is possible to assume without loss of generality that the fixed frame $\mathcal{F}_O$ is coincident with $\mathcal{F}_T$, which means that $\boldsymbol{P} = [0, 0, 0, 1]^T$ and $\boldsymbol{E} \equiv \boldsymbol{Q}$.

Given the preceding statements and definitions, it is easy to express the quaternion associated with the desired rotation $\mathcal{R}_{\text{des}}(\hat{\boldsymbol{e}}, \phi)$ that takes $\mathcal{F}_B$ from its initial position represented by $\boldsymbol{Q}_1$ onto the target attitude $\mathcal{F}_T$ represented by the quaternion $\boldsymbol{P}$ as the conjugate of the (initial) quaternion error vector (Fig. 1b):

$$\boldsymbol{R}_{\text{des}} = [\hat{\boldsymbol{e}}^T \sin(\phi/2), \cos(\phi/2)]^T = \boldsymbol{Q}_1^*\boldsymbol{P}$$

where the unit vector $\hat{\boldsymbol{e}}$ is represented in the current body-axes frame $\mathcal{F}_B$.

When there is an axis $\hat{\boldsymbol{b}}$, around which it is not possible to obtain a component for the rotation (e.g., for the considered applicative scenario, when a spacecraft is underactuated and its control hardware cannot deliver a control torque component around an axis $\hat{\boldsymbol{b}}$) $\hat{\boldsymbol{e}}$ may not be a feasible rotation axis, so that in the most general case it is not possible to perform the desired maneuver around $\hat{\boldsymbol{e}}$. A feasible rotation axis $\hat{\boldsymbol{g}}$, perpendicular to $\hat{\boldsymbol{b}}$, must thus be chosen such that the feasible rotation $\mathcal{R}(\hat{\boldsymbol{g}}, \hat{\phi})$ takes $\mathcal{F}_B$ onto a different final attitude represented by $\boldsymbol{Q}_2$. The quaternion error vector $\boldsymbol{E}$ after the feasible rotation around $\hat{\boldsymbol{g}}$ is given by

$$\boldsymbol{E} = \boldsymbol{P}^*\boldsymbol{Q}_2 = \boldsymbol{P}^*(\boldsymbol{Q}_1\boldsymbol{R}) = (\boldsymbol{P}^*\boldsymbol{Q}_1)\boldsymbol{R} = \boldsymbol{R}_{\text{des}}^*\boldsymbol{R}$$

where $\boldsymbol{R} = [\hat{\boldsymbol{g}}^T \sin(\hat{\phi}/2), \cos(\hat{\phi}/2)]^T$. By use of the quaternion multiplication rule [Eq. (1)], one can thus express the final

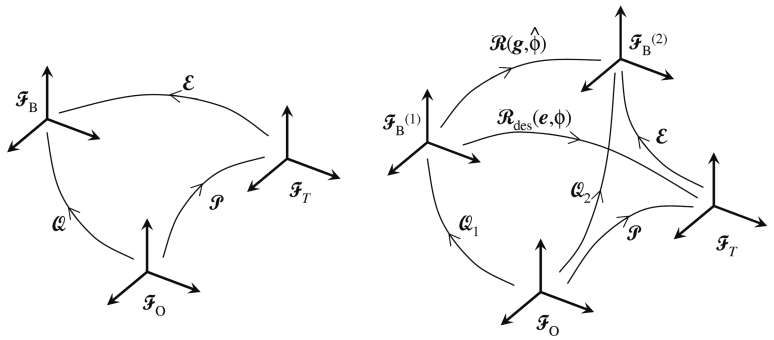

a) b)

Fig. 1 Definition of a) quaternion error and b) desired and admissible rotations.

misalignment from the fourth component of the quaternion error vector expressed as

$$\bar{\epsilon} = \cos(\varepsilon/2) = \cos(\hat{\phi}/2)\cos(\phi/2) + (\hat{\boldsymbol{e}} \cdot \hat{\boldsymbol{g}})\sin(\hat{\phi}/2)\sin(\phi/2) \tag{2}$$

that is,

$$\varepsilon = 2\cos^{-1}[\cos(\hat{\phi}/2)\cos(\phi/2) + (\hat{\boldsymbol{e}} \cdot \hat{\boldsymbol{g}})\sin(\hat{\phi}/2)\sin(\phi/2)] \tag{3}$$

Figure 2 represents $\varepsilon(\hat{\phi})$ expressed by Eq. (3), plotted for various values of the scalar product $\hat{\boldsymbol{e}} \cdot \hat{\boldsymbol{g}}$ and a fixed desired eigenaxis rotation amplitude $\phi = 70$ deg, as in [27]. As expected, the plots match exactly, but the derivation carried out with the quaternion approach is significantly more straightforward and intuitive.

The nonnominal rotation angle $\hat{\phi}$ that results in the minimum value for the misalignment error, ε, is evaluated analytically as in [27] by maximizing $\bar{\epsilon} = \cos(\varepsilon/2)$. The derivative $\mathrm{d}\bar{\epsilon}/\mathrm{d}\hat{\phi}$, obtained from (3), vanishes for

$$\hat{\phi}_{\text{opt}} = 2\tan^{-1}[(\hat{\boldsymbol{e}} \cdot \hat{\boldsymbol{g}})\tan(\phi/2)] \tag{4}$$

The second derivative $\mathrm{d}^2\bar{\epsilon}/\mathrm{d}\hat{\phi}^2$ is always negative for $\hat{\phi} = \hat{\phi}_{\text{opt}}$, thus proving that $\hat{\phi}_{\text{opt}}$ provides a maximum for $\bar{\epsilon}$. Upon substitution of the value of $\hat{\phi}_{\text{opt}}$ in Eq. (3), the minimum value of ε is expressed as

$$\varepsilon_{\min} = 2\cos^{-1}[\cos^2(\phi/2) + (\hat{\boldsymbol{e}} \cdot \hat{\boldsymbol{g}})^2\sin^2(\phi/2)]^{1/2} \tag{5}$$

The dashed line in Fig. 2 represents the optimal rotations $\hat{\phi}_{\text{opt}}$ in the given situation, and it intersects all the minima of the curves. The minimum misalignment $\varepsilon_{\min}$ attainable as a function of the desired rotation angle ϕ for different values of $\hat{\boldsymbol{e}} \cdot \hat{\boldsymbol{g}}$ is reported in Fig. 3. The reported results clearly show how the final error grows with the angle between the desired and actual rotation axes, $\hat{\boldsymbol{e}}$ and $\hat{\boldsymbol{g}}$, so that the best admissible axis $\hat{\boldsymbol{g}}$ is obtained when such an angle is minimum, that is, when $\hat{\boldsymbol{g}}$ is parallel to the projection of $\hat{\boldsymbol{e}}$ onto the plane of admissible rotations [27]. Moreover, ε grows linearly for small angular displacements, becoming equal to $\cos^{-1}(\hat{\boldsymbol{e}} \cdot \hat{\boldsymbol{g}})$ for $\phi = 180$ deg. This clearly shows that, unless the desired rotation angle is small, the misalignment becomes soon considerable when the angle between $\hat{\boldsymbol{e}}$ and $\hat{\boldsymbol{g}}$ is greater than few degrees, resulting unacceptable for any practical application if large slews are to be tracked.

Exact Pointing with Two Rotations

Problem Statement and Preliminary Considerations

In this section it will be shown that, in the presence of a constraint on admissible rotation axes, it is nonetheless possible to achieve any desired attitude $\mathcal{F}_T$ by means of two successive admissible rotations only, $\mathcal{R}_1(\hat{\boldsymbol{g}}_1, \hat{\phi}_1)$ and $\mathcal{R}_2(\hat{\boldsymbol{g}}_2, \hat{\phi}_2)$, regardless of the fact that the torqueless direction $\hat{\boldsymbol{b}}$ is prescribed in either the fixed frame $\mathcal{F}_O$ (case 1) or in body axes $\mathcal{F}_B$ (case 2). This latter aspect was not relevant in the previous works on kinematic approaches for maneuver planning of underactuated satellites [27,28], inasmuch as a single nonnominal eigenaxis rotation was considered in both cases, such that the angle between the admissible rotation axis $\hat{\boldsymbol{g}}$ and the torqueless direction $\hat{\boldsymbol{b}}$ was constant during the maneuver. On the converse, when two rotations are considered, the position of the plane of admissible axes after the first one will depend on whether $\hat{\boldsymbol{b}}$ is constant in $\mathcal{F}_O$ or $\mathcal{F}_B$.

In what follows, three coordinate frames will be considered:

1) A fixed frame $\mathcal{F}_O$ that, without loss of generality, can be assumed as coincident with the initial position of the body frame $\mathcal{F}_B^{(0)}$.

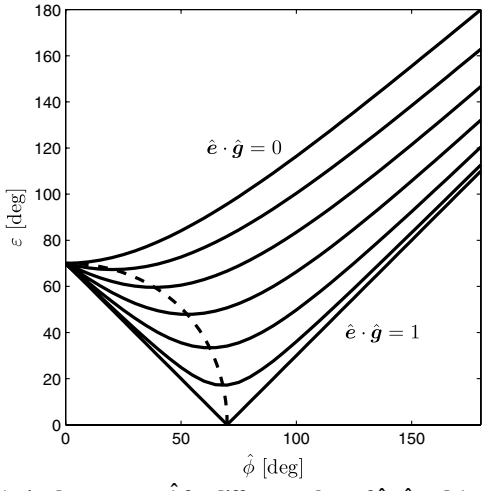

Fig. 2 Attitude error ε vs $\hat{\phi}$ for different values of $\hat{\boldsymbol{e}} \cdot \hat{\boldsymbol{g}}$ and $\phi = 70$ deg [27].

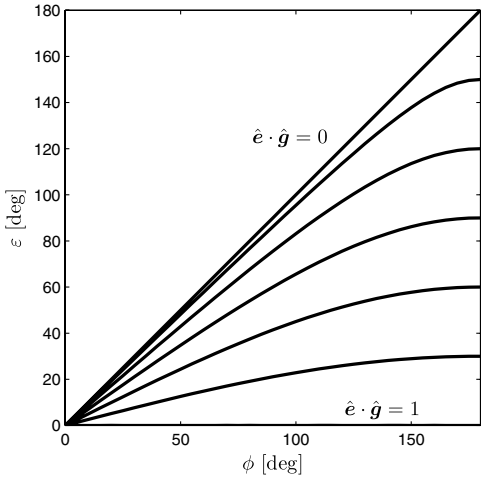

Fig. 3 Minimum attitude error $\varepsilon_{\min}$ vs ϕ for different values of $\hat{\boldsymbol{e}} \cdot \hat{\boldsymbol{g}}$.

2) An intermediate position for the body frame, $\mathcal{F}_B^{(1)}$, after the first rotation.

3) The final position of the body frame, $\mathcal{F}_B^{(2)}$, that should coincide with the target frame, $\mathcal{F}_T$.

In both case 1 and 2, the first rotation must move the axis of the quaternion error vector onto the plane of admissible rotation axes Γ, perpendicular to $\hat{\boldsymbol{b}}$. The problem of identifying the sequence of two admissible rotations will thus be solved by showing that, for any admissible axis $\hat{\boldsymbol{g}}_1 \in \Gamma$ used for performing the first step of the maneuver, it is always possible to identify a rotation angle $\hat{\phi}_1$ such that the direction $\boldsymbol{\epsilon}$ of the vector part of the quaternion error after the first rotation lies on Γ. By choosing $\boldsymbol{\epsilon}$ as the second admissible rotation axis, a feasible second rotation can be obtained that takes $\mathcal{F}_B$ onto the desired target frame $\mathcal{F}_T$, its amplitude being simply given by

$$\varepsilon = 2\cos^{-1}(\bar{\epsilon}) \tag{6}$$

Again without loss of generality, the following will be also assumed:

1) The attitude control hardware cannot deliver a torque component around $\hat{\boldsymbol{b}} \equiv \hat{\boldsymbol{e}}_3^{(0)}$, that is, the plane of admissible rotations Γ is perpendicular to the initial position of the third body axis, $\hat{\boldsymbol{e}}_3$.

2) The initial position of the body axis $\hat{\boldsymbol{e}}_1^{(0)}$ lies along the projection of the desired nominal Euler rotation eigenaxis $\hat{\boldsymbol{e}}$ on Γ.

3) The unit vector $\hat{\boldsymbol{e}}_2^{(0)}$ completes a right-handed triad $\mathcal{F}_B^{(0)}$.

Even though this peculiar choice of axes for $\mathcal{F}_B^{(0)}$ may appear as a particular case, a simple coordinate transformation is sufficient for rotating any arbitrary (and possibly more standard) choice for the body-axes frame onto $\mathcal{F}_B^{(0)}$, similarly to what was done in [28]. Note also that $\hat{\boldsymbol{e}}_1^{(0)}$ lies along the direction of the optimal admissible rotation axis identified in [27].

The angle λ between $\hat{\boldsymbol{b}}$ and $\hat{\boldsymbol{e}}$ is used in order to identify the direction of the eigenaxis for the desired maneuver. Note that, with a proper choice of the direction of $\hat{\boldsymbol{b}}$, it is always $\lambda \in [0, \pi/2]$. The direction of $\hat{\boldsymbol{e}}_1^{(0)}$ is used in order to identify the admissible rotation axes on Γ by means of the angles α_i, $i = 1, 2$, between $\hat{\boldsymbol{g}}_i$ and $\hat{\boldsymbol{e}}_1^{(0)}$ itself, when $\hat{\boldsymbol{b}}$ and Γ are fixed in $\mathcal{F}_O$, while the angle α_i lies between $\hat{\boldsymbol{g}}_i$ and $\hat{\boldsymbol{e}}_1^{(i-1)}$, when $\hat{\boldsymbol{b}}$ and Γ are fixed in $\mathcal{F}_B$.

Under the preceding hypotheses, the direction of the relevant unit vectors can be easily expressed in $\mathcal{F}_O$, where the torqueless direction is $\hat{\boldsymbol{b}} = [0, 0, 1]^T$ and the desired Euler axis is defined as $\hat{\boldsymbol{e}} = [\sin\lambda, 0, \cos\lambda]^T$. Feasible rotation axes $\hat{\boldsymbol{g}}_i$ lying on the plane Γ can be expressed as $\hat{\boldsymbol{g}}_i = [\cos\alpha_i, \sin\alpha_i, 0]^T$ in either $\mathcal{F}_O$ or $\mathcal{F}_B$, depending on whether $\hat{\boldsymbol{b}}$ is prescribed in the fixed or in the body frame.

Assuming that the quaternion

$$\begin{aligned}\boldsymbol{P} &= [\boldsymbol{p}^T, \bar{p}]^T = [\hat{\boldsymbol{e}}^T \sin\phi/2, \cos\phi/2]^T \\ &= [\sin(\phi/2)\sin\lambda, 0, \sin(\phi/2)\cos\lambda, \cos\phi/2]^T\end{aligned} \tag{7}$$

associated to the desired rotation $\mathcal{P}(\hat{\boldsymbol{e}}, \phi)$ describes the position of the target frame, the quaternions $\boldsymbol{R}_1$ and $\boldsymbol{R}_2$ associated to the two feasible rotations must satisfy the equation

$$\boldsymbol{P} = \boldsymbol{R}_1 \boldsymbol{R}_2 \tag{8}$$

According with the quaternion-based formulation, the quaternion $\boldsymbol{R}1$ associated to the first feasible rotation $\mathcal{R}_1(\hat{\boldsymbol{g}}_1, \hat{\phi}_1)$ coincides with the quaternion representing the position of $\mathcal{F}_B$ with respect to $\mathcal{F}_O$ after the first rotation, that is,

$$\begin{aligned}\boldsymbol{R}_1 \equiv \boldsymbol{Q}_1 &= [\boldsymbol{q}^T, \hat{q}_1]^T = [\hat{\boldsymbol{g}}_1 \sin(\hat{\phi}_1/2), \cos(\hat{\phi}_1/2)]^T \\ &= [\sin(\hat{\phi}_1/2)\cos\alpha_1, \sin(\hat{\phi}_1/2)\sin\alpha_1, 0, \cos(\hat{\phi}_1/2)]^T\end{aligned} \tag{9}$$

where $\hat{\boldsymbol{g}}_1$ and $\hat{\phi}_1$ are the first feasible rotation axis and angle, respectively.

Once the first rotation is performed, the attitude error is described by the quaternion error vector given by the product

$$\boldsymbol{E} = [\boldsymbol{\epsilon}^T, \bar{\epsilon}]^T = \boldsymbol{P}^* \boldsymbol{Q}_1 \tag{10}$$

where, as stated previously, $\boldsymbol{\epsilon}$ provides the direction of the desired Euler axis for the second rotation, described by the quaternion

$$\boldsymbol{R}_2 = [\boldsymbol{r}_2^T, \bar{r}_2] = \boldsymbol{E}^* = \boldsymbol{Q}_1^* \boldsymbol{P} \tag{11}$$

The quaternion $\boldsymbol{R}_2$ represents a feasible rotation if its vector part

$$\boldsymbol{r}_2 = \bar{q}_1 \boldsymbol{p} - \bar{p}\boldsymbol{q}_1 - \boldsymbol{q}_1 \times \boldsymbol{p} \tag{12}$$

lies on the Γ plane, that is, if $\boldsymbol{r}_2$ is perpendicular to $\hat{\boldsymbol{b}}$,

$$\hat{\boldsymbol{b}} \cdot \boldsymbol{r}_2 = 0 \tag{13}$$

where the constraint represented by Eq. (13) must be formulated in different ways, depending on whether case 1 or 2 is dealt with.

Analytical Solution for Case 1: $\hat{\boldsymbol{b}}$ Constant in the Fixed Frame $\mathcal{F}_O$

The components of the eigenaxis parallel to $\boldsymbol{r}_2$ of the Euler rotation that takes the body frame onto the target frame and parallel to vector part of the quaternion error vector after the first rotation, $\boldsymbol{\epsilon}$, are expressed in either one of these two frames. When the torqueless direction $\hat{\boldsymbol{b}}$ is prescribed in the fixed frame $\mathcal{F}_O$ it is necessary to project the coordinates of $\boldsymbol{r}_2$ from $\mathcal{F}_B$ in $\mathcal{F}_O$ by means of the coordinate transformation matrix $\mathbb{T}_{OB}^{(1)}$, in order to enforce the constraint expressed by Eq. (13), which is thus rewritten as

$$\hat{\boldsymbol{b}}(\mathbb{T}_{OB}^{(1)}\boldsymbol{r}_2) = \hat{\boldsymbol{b}}^T(\mathbb{T}_{BO}^{(1)})^T\boldsymbol{r}_2 = 0 \tag{14}$$

where [26]

$$\mathbb{T}_{BO}^{(1)} = (\bar{q}_1^2 - \boldsymbol{q}_1^T\boldsymbol{q}_1)\mathbb{I} + 2\boldsymbol{q}_1\boldsymbol{q}_1^T - 2\bar{q}_1\mathbb{Q}_1^{\times}$$

with $\mathbb{I}$ and $\mathbb{Q}_1^{\times}$ representing the 3×3 identity matrix and the skew symmetric matrix equivalent for the cross product of $\boldsymbol{q}_1$, respectively.

Upon substitution of Eq. (12) into Eq. (14), one gets after some manipulations

$$(\mathbb{T}_{BO}^{(1)})^T\boldsymbol{r}_2 = \bar{q}_1\boldsymbol{p} - \bar{p}\boldsymbol{q}_1 + \boldsymbol{q}_1 \times \boldsymbol{p} \equiv \boldsymbol{r}_O \tag{15}$$

Remembering that $\boldsymbol{b} = [0, 0, 1]^T$, the scalar product is simply obtained from the third component of the vector $\boldsymbol{r}_O$, so that, introducing the definitions of $\boldsymbol{Q}_1$ and $\boldsymbol{P}$ from Eqs. (9) and (7), respectively, into Eq. (15), Eq. (14) can be expressed in the form

$$\cos(\hat{\phi}_1/2)\cos\lambda - \sin(\hat{\phi}_1/2)\sin\alpha_1\sin\lambda = 0 \tag{16}$$

From the latter equation it is clear that, for any given λ and for any choice of α_1, there exists an angle $\hat{\phi}_1$ such that

$$\tan(\hat{\phi}_1/2) = \frac{\cos\lambda}{\sin\alpha_1\sin\lambda} \tag{17}$$

thus satisfying Eq. (16) independently of the amplitude ϕ of the nominal Euler eigenaxis rotation. To avoid singularities, the value of $\hat{\phi}_1$ is obtained in the form

$$\hat{\phi}_1 = 2\tan^{-1}(\cos\lambda, \sin\alpha_1\sin\lambda) \tag{18}$$

where $\tan^{-1}(y, x)$ is the four-quadrant inverse tangent function. Note that it is possible to limit the variation of α_1 to the interval $[0, \pi]$ rad, as negative values would result in the same rotation axis pointing in the opposite direction, with an opposite value of $\hat{\phi}_1$. Within these limits, all the arguments of the inverse tangent function are positive, so that a positive value of $\hat{\phi}_1 \in [0, \pi]$ rad is expected. An example for $\lambda = 5\pi/18$ rad $= 50$ deg and $\alpha = 7\pi/18$ rad $= 70$ deg is depicted in Fig. 4, where the variation of the direction of the quaternion error vector (continuous segments) for rotations $\hat{\phi}_1 \in [0, \pi]$ rad

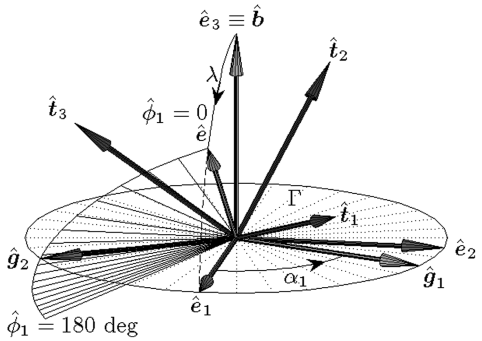

Fig. 4 Direction of the quaternion error axis for different values of $\hat{\phi}_1 \in [0; 180]$ deg ($\lambda = 50$ deg, $\phi = 70$ deg, $\alpha_1 = 70$ deg).

around $\hat{g}_1$ is reported (with increments $\Delta\hat{\phi}_2 = \pi/18$ rad $= 10$ deg). For $\hat{\phi}_1 = 1.46$ rad ≈ 83.5 deg a feasible position for $\hat{g}_2$ on the plane of feasible rotations Γ (dotted circle perpendicular to $\hat{b} \equiv \hat{e}_3$) is achieved. The variation of $\hat{\phi}_1$ with $\alpha_1 \in [0, \pi]$ rad for different values of $\lambda \in [0, \pi/2]$ rad is reported in Fig. 5.

After performing the rotation $\mathcal{R}_1(\hat{g}_1, \hat{\phi}_1)$, a second feasible rotation $\mathcal{R}_2(\hat{g}_2, \hat{\phi}_2)$ is obtained by choosing

$$\hat{g}_2 = r_O/\|r_O\|, \qquad \hat{\phi}_2 = 2\text{sign}(\bar{r}_2)\cos^{-1}(|\bar{r}_2|) \tag{19}$$

where

$$\bar{r}_2 = \bar{q}_1\bar{p} + q_1^T p$$
$$= \cos(\phi/2)\cos(\hat{\phi}_1/2) + \sin(\phi/2)\sin(\hat{\phi}_1/2)\sin\lambda\cos\alpha_1$$

is the fourth component of the quaternion error vector. The expression for the amplitude of the second rotation, $\hat{\phi}_2$, in Eq. (19) is formulated so as to consider only rotation angles smaller than π. By enforcing Eq. (16), the third component of r_O is zero and the direction of $\hat{g}_2$ on the plane Γ can be expressed by means of the angle

$$\alpha_2 = \tan^{-1}(r_{O_2}, r_{O_1}) \tag{20}$$

where the components of $r_O = [r_{O_1} r_{O_2} 0]^T$ are obtained by substituting Eq. (17) into Eq. (15) and a four-quadrant inverse tangent function is again adopted.

The complete sequence of the two-step maneuver for the example considered ($\lambda = 50$ deg and $\phi = 70$ deg) is represented in Fig. 6, where the maneuver is completed by means of a rotation $\hat{\phi}_2 = 1.56$ rad ≈ 89.4 deg around $\hat{g}_2$ ($\alpha_2 = -1.01$ rad ≈ -58 deg). The total angular travel necessary for performing the desired maneuver is thus equal to 172.9 deg, much wider than the amplitude of the ideal eigenaxis rotation around the desired eigenaxis (70 deg only), but the considered rotations are now feasible ones.

Note that, in general, Eq. (20) can provide results for α_2 anywhere in the interval $[-\pi, \pi]$, that is, $\hat{g}_2$ can lie anywhere on Γ, provided that

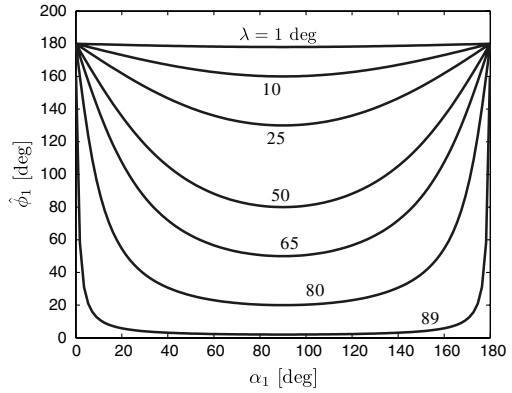

Fig. 5 Variation of $\hat{\phi}_1$ with α for different values of λ.

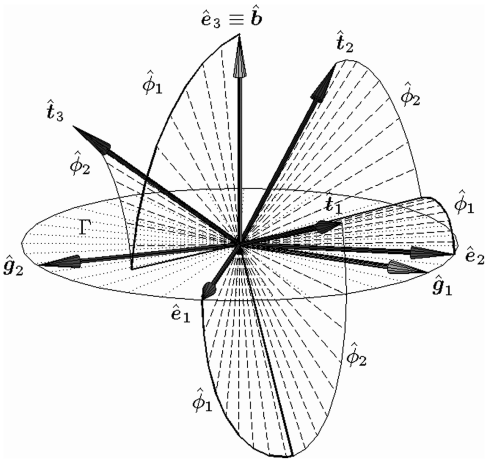

Fig. 6 Sequence of two rotations that overlaps $\mathcal{F}_B$ onto $\mathcal{F}_T$ ($\lambda = 50$ deg, $\phi = 70$ deg, $\alpha_1 = 70$ deg).

$\hat{\phi}_2 > 0$ when $\alpha_2 < 0$ and vice versa. Moreover, the value of $\hat{\phi}_2$ "jumps" from π rad to $-\pi$ when the threshold $\alpha_2 = 0$ is crossed. These features are clearly demonstrated by the example shown in Fig. 7, where the variation of $\hat{\phi}_2$ (continuous line) and α_2 (dashed line) with α_1 for $\lambda = 5\pi/18$ rad $= 50$ deg is reported for different values of the amplitude of the nominal eigenaxis rotation, ϕ. The corresponding variation of $\hat{\phi}_1$ is also shown (dotted line), which does not depend on ϕ, as already shown previously by Eq. (17).

Solution for Minimum Angular Travel

The total angular travel $|\hat{\phi}_1| + |\hat{\phi}_2|$ for completing the maneuver is reported in Fig. 8, for the same cases considered in Fig. 7, where the presence of an optimal choice of α_1, resulting in the minimum angular travel two-rotation sequence is evident. This value will be determined analytically by minimizing the cost function:

$$J_{\hat{\phi}} = |\hat{\phi}_1| + |\hat{\phi}_2| \tag{21}$$

where, due to the constraint represented by Eq. (16), the cost function $J_{\hat{\phi}}$ depends on α_1 only, that is, one can write $J_{\hat{\phi}} = f(\alpha_1)$, in compact form.

As shown in the previous paragraph, $\hat{\phi}_1 \in [0, \pi]$, that is, it is strictly positive, so that the first absolute value sign in Eq. (21) can be removed. On the converse $\hat{\phi}_2 \in [-\pi, \pi]$ may be negative or positive. It should be noted that the jump in the value of $\hat{\phi}_2$ when $\alpha_2 = 0$ results into a discontinuity for the first derivative of $J_{\hat{\phi}}$ with respect to α_1 (Fig. 7).

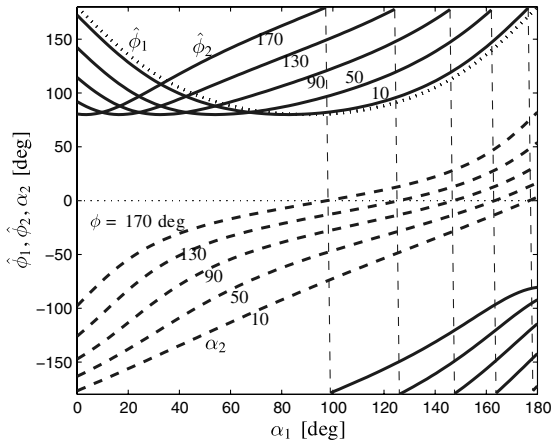

Fig. 7 Variation of $\hat{\phi}_2$ and α_2 with α_1 for $\lambda = 50$ deg and different values of ϕ.

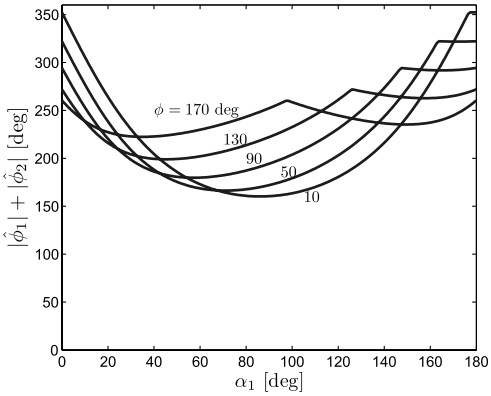

Fig. 8 Total angular travel for $\lambda = 50$ deg and different values of ϕ.

The value of α_1 which minimizes the angular travel can be found by setting to zero the derivative of $J_{\hat{\phi}}$ with respect to α_1:

$$\frac{\mathrm{d}J_{\hat{\phi}}}{\mathrm{d}\alpha_1} = 0 \tag{22}$$

where the explicit expression of $J_{\hat{\phi}}$ as a function of the position of the first feasible rotation axis, α_1, and problem parameters (λ and ϕ) is obtained by substituting the values of $\hat{\phi}_1$ and $\hat{\phi}_2$ obtained in the previous paragraph. When $\alpha_2 < 0$ and $\phi_2 < 0$ it is

$$J_{\hat{\phi}} = 2\tan^{-1}\left[\frac{1}{\sin\alpha_1 \tan\lambda}\right] + 2\cos^{-1}\left[\frac{\cos(\phi/2)\sin\alpha_1\tan\lambda + \sin(\phi/2)\sin\lambda\cos\alpha_1}{\sin\alpha_1\tan\lambda\sqrt{1+1/(\sin^2\alpha_1\tan^2\lambda)}}\right] \tag{23}$$

and the analytical solution of Eq. (22) is

$$\tan\alpha_1 = \frac{\sin(\phi/2)\cos\lambda}{1-\cos(\phi/2)} \tag{24}$$

The corresponding value of $\hat{\phi}_2$ is obtained by considering that, from Eq. (16), one has

$$\sin(\hat{\phi}_1/2) = \frac{\cos(\hat{\phi}_1/2)}{\sin\alpha_1\tan\lambda} \tag{25}$$

Taking into account the result given by Eq. (24), substitution of the last relation into Eq. (19) leads to

$$\cos(\hat{\phi}_2/2) = \left[\cos(\phi/2) + \sin(\phi/2)\cos\lambda\frac{1-\cos(\phi/2)}{\sin(\phi/2)\cos\lambda}\right] \times \cos(\hat{\phi}_1/2) = \cos(\hat{\phi}_1/2) \tag{26}$$

that is, the minimum angular travel solution results into equal rotations, $\hat{\phi}_2 = \hat{\phi}_1$, as they were assumed to be both positive. By means of a rather cumbersome derivation (not reported for the sake of conciseness) it is also possible to show that, in this condition, it is $\alpha_2 = -\alpha_1$, that is, the feasible rotation axes $\hat{\boldsymbol{g}}_1$ and $\hat{\boldsymbol{g}}_2$ are placed symmetrically with respect to the projection of $\hat{\boldsymbol{e}}$ on the plane Γ. The minimum angular travel solution can be easily determined graphically, from plots like those reported in Fig. 7, where, thanks to the previous results, the optimal value of α_1 is obtained from the intersection of the dotted line representing $\hat{\phi}_1$ with the continuous ones, that illustrates the variation of $\hat{\phi}_2$.

It is possible to show that, when α_2 is positive and $\hat{\phi}_2$ is negative a minus sign appears between the two terms in Eq. (23), because of the absolute sign in Eq. (22). The resulting local minimum is for

$$\tan\alpha_1 = -\frac{\sin(\phi/2)\cos\lambda}{1+\cos(\phi/2)}$$

with $\hat{\phi}_2 = -\hat{\phi}_1$ and $\alpha_2 = \pi - \alpha_1$. But when α_1 and α_2 have the same sign in the framework of the formulation here adopted, the resulting minimum is only local, the sum of the absolute values of the rotation amplitudes being always higher than in the previous case, when the rotation axes lie on opposite sides of $\hat{\boldsymbol{e}}_1$ and the rotations are both positive. The proof can be obtained by means of elementary goniometric considerations, omitted for the sake of conciseness.

Analytical Solution for Case 2: $\hat{\boldsymbol{b}}$ Constant in the Body Frame $\mathcal{F}_B$

When the torqueless direction $\hat{\boldsymbol{b}}$ is prescribed in the body frame $\mathcal{F}_B$ both vectors in Eq. (13) are already expressed in $\mathcal{F}_B$, so that the orthogonality condition between $\boldsymbol{r}_2$ and $\boldsymbol{b}$ is enforced by setting the third component of $\boldsymbol{r}_2$ as obtained from Eq. (12) equal to 0, that is,

$$\cos(\hat{\phi}_1/2)\cos\lambda + \sin(\hat{\phi}_1/2)\sin\alpha_1\sin\lambda = 0 \tag{27}$$

The amplitude of the first rotation that achieves a feasible position for the direction of the vector part of the quaternion error thus satisfies the following equation:

$$\tan(\hat{\phi}_1/2) = -\frac{\cos\lambda}{\sin\alpha_1\sin\lambda} \tag{28}$$

and it can be expressed as

$$\hat{\phi}_1 = -2\tan^{-1}(\cos\lambda, \sin\alpha_1\sin\lambda) \tag{29}$$

that is, under the hypotheses stated preceding, a negative rotation is obtained. Exactly as for case 1, a second feasible rotation $\mathcal{R}_2(\hat{\boldsymbol{g}}_2, \hat{\phi}_2)$ for case 2 can now be performed by choosing

$$\hat{\boldsymbol{g}}_2 = \boldsymbol{r}_O/\|\boldsymbol{r}_O\|, \qquad \hat{\phi}_2 = 2\cos^{-1}(\bar{r}_2)$$

where $\bar{r}_2 = \bar{q}_1\bar{p} + \boldsymbol{q}_1^T\boldsymbol{p}$ is the scalar part of the quaternion error vector. The direction of $\hat{\boldsymbol{g}}_2$ on Γ is represented by the angle

$$\alpha_2 = \tan^{-1}(r_{O_2}, r_{O_1}) \tag{30}$$

and $\hat{\phi}_2$ is given by

$$\hat{\phi}_2 = 2\cos^{-1}[\cos(\phi/2)\cos(\hat{\phi}_1/2) + \sin(\phi/2)\sin(\hat{\phi}_1/2)\sin\lambda\cos\alpha_1] \tag{31}$$

Note that the derivation necessary for determining the minimum angular travel solution for case 2 is formally almost identical to that presented for case 1, with just a few changes of sign, and it is thus not repeated.

Optimal Sequences of N Rotations

Problem Statement in Terms of an Unconstrained Minimization Process

Provided that two rotations are always sufficient for reaching any target attitude $\boldsymbol{P}$, it is now possible to generalize the problem to the determination of a sequence of $N > 2$ feasible rotations $\mathcal{R}_i(\hat{\boldsymbol{g}}_i, \hat{\phi}_i)$, $i = 1, 2, \ldots, N$, each one described by a feasible rotation axis $\hat{\boldsymbol{g}}_i \in \Gamma$ and the corresponding rotation amplitude $\hat{\phi}_i$. The optimal sequence that results in the minimum overall angular travel will be determined by means of a numerical optimization approach, in order to highlight the properties of the optimal sequences for increasing values of N.

Under the same initial hypotheses stated for $N = 2$, it is possible to express the final attitude $\boldsymbol{Q}_N$ achieved after N rotations as

$$\boldsymbol{Q}_N = \boldsymbol{R}_1\boldsymbol{R}_2\ldots\boldsymbol{R}_{N-1}\boldsymbol{R}_N$$

where the quaternion error vector after the sequence is given by $\boldsymbol{E}_N = (\boldsymbol{\epsilon}_N^T, \bar{\epsilon}_N) = \boldsymbol{P}^*\boldsymbol{Q}_N$. Each rotation is described by means of two parameters, namely the angle α_i that prescribes the direction on Γ of the ith feasible rotation axis, and the corresponding rotation amplitude $\hat{\phi}_i$. Rather than minimizing the total angular travel

$$J_{\hat{\phi}} = \phi_{\text{tot}} = \sum_{i=1}^{N} |\hat{\phi}_i| \tag{32}$$

expressed as a function of $2N$ parameters and subject to three constraints:

$$\boldsymbol{\epsilon}_N = (0, 0, 0)^T$$

the analytical solution for a two-rotation sequence previously derived can be exploited for reducing the size of the search space and, more important, to enforce the constraints, thus reducing the optimization problem to an unconstrained minimization.

The sequence of N rotations is split into two parts (Fig. 9):

1) An initial sequence of $N-2$ feasible rotations, that drives the frame $\mathcal{F}_B$ from its initial position $\mathcal{F}_B^{(0)} = \mathcal{F}_O$ to $\mathcal{F}_B^{(N-2)}$.

2) A final sequence of two rotations that, by a proper choice of $\hat{\phi}_{N-1}$, α_N, and $\hat{\phi}_N$ as a function of α_{N-1}, completes the desired maneuver by taking $\mathcal{F}_B$ from $\mathcal{F}_B^{(N-2)}$ over $\mathcal{F}_B^{(N)} \equiv \mathcal{F}_T$.

This means that, if on one side the parameters α_i and $\hat{\phi}_i$ for $i < N-1$ can be assigned arbitrarily, on the other hand the only free parameter left for the remaining sequence of two rotations is the position α_{N-1} of the axis $\hat{\boldsymbol{g}}_{N-1}$. The rest of the data for the sequence can be determined by means of the technique described in the previous paragraph, as for any given value of α_{N-1}, it is possible to determine a rotation amplitude $\hat{\phi}_{N-1}$ such that the $(N-1)$th rotation will result into a quaternion error vector $\boldsymbol{E}_{N-1} = \boldsymbol{P}^* \boldsymbol{Q}_{N-1}$, the vector part of which is a feasible rotation axis. Thus, by assuming $\hat{\phi}_N = 2\cos^{-1}(\bar{\epsilon}_{N-1})$ and $\hat{\boldsymbol{g}}_N = -\boldsymbol{\epsilon}_{N-1}/\|\boldsymbol{\epsilon}_{N-1}\|$ one completes the desired reorientation. The constraint $\boldsymbol{\epsilon}_N = (0, 0, 0)^T$ is thus enforced while evaluating the total angular travel as

$$J_{\hat{\phi}} = \sum_{i=1}^{N-2} |\hat{\phi}_i| + |\hat{\phi}_{N-1}(\alpha_{N-1})| + |\hat{\phi}_N(\alpha_{N-1})| = \boldsymbol{f}(\boldsymbol{x}) \tag{33}$$

where the search space for the unconstrained minimization of $J_{\hat{\phi}}$ is defined by the vector

$$\boldsymbol{x} = (\alpha_1, \hat{\phi}_1, \alpha_2, \hat{\phi}_2, \ldots, \alpha_{N-2}, \hat{\phi}_{N-2}, \alpha_{N-1})^T \in \mathbb{R}^{2N-3}$$

Numerical Optimization and Related Issues

A sequential-quadratic algorithm (SQP) can successfully tackle the problem of minimizing $J_{\hat{\phi}}$, which is a smooth function of $\boldsymbol{x}$ within all the basins of attractions of each local minima. Convergence is fast, but quite obviously the local minimum found will depend on the initial guess adopted. It was previously shown that, for the $N = 2$ case, the total angular travel always features two local minima, one of the two being the true global optimal sequence. For a larger search space an increasing number of local minima is expected.

This fact was confirmed by use of a simple MS approach, for a random definition of a large set of initial guesses (200 samples randomly distributed over the entire search space). Moreover, this preliminary analysis highlighted how many minima of $J_{\hat{\phi}}$ for $N = N_A$ are also a local minimum for $J_{\hat{\phi}}$, when a higher number of rotations $N = N_B > N_A$ is considered. When this happens, $N_B - N_A$ rotations of the larger sequence have zero amplitude at convergence. As a major drawback of this situation, the corresponding value of α_i does not affect the optimality of the solution and convergence to the local optimum can become ill conditioned.

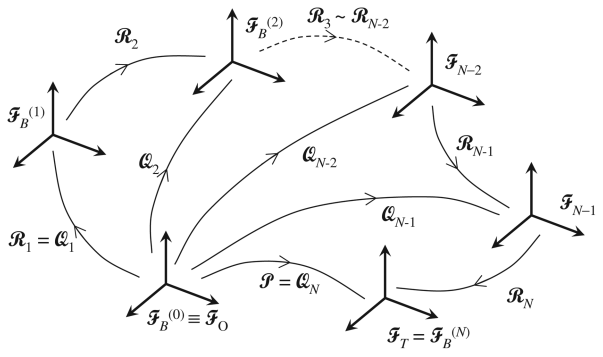

Fig. 9 Sequence of N admissible rotations $\mathcal{R}_i$ that exactly reaches the target frame $\mathcal{F}_T$.

Thus, on one side, a straightforward application of the SQP approach hardly achieves the local optimum but for a few initial lucky guesses, on the other one, a massive computation is required, when one wants to scan the whole space in search of the global optimum. The problem is not relevant for $N = 2$, where an analytical solution was obtained, or $N = 3$, when most of the runs (approximately 93%) converge to the absolute minimum. But even for $N = 3$, as many as five different local minima were found, three of which were two-step maneuvers with either one of the three rotation amplitudes brought to zero.

When a sequence of $N = 4$ rotations is adopted for obtaining the equivalent desired rotation $\phi = 30$ deg around an eigenaxis only $\lambda = 20$ deg away from the torqueless direction $\hat{\boldsymbol{b}}$, as many as 26 different local minima with 4 nonzero rotations were found over 200 runs, the optimal sequences with one or more zero rotations having been dropped during the postprocessing phase. These solutions are reported in Table 1, where the global optimum featuring the absolute minimum for $J_{\hat{\phi}}$ is the first solution and the other ones are listed for increasing values of the performance index. Note that many local minima present a minor penalty with respect to the global optimum, the position of the axes and the amplitude of the rotations being sufficiently close to the best solution found.

The global optima for $N = 2, 3$ and 4 already show two interesting properties:

1) The rotations of the optimal sequence are equal in amplitude.

2) The admissible rotation axes are placed symmetrically with respect to their reference position, $\alpha = 0$, that is, the projection of the eigenaxis $\hat{\boldsymbol{e}}$ of the desired rotation on the plane Γ of admissible axes. But as shown by the results reported in Table 1, the optimal sequence lies in a region of the search space where the merit function is relatively flat, with many basins of attractions of small size, each one driving the solution towards a local optimum. The presence of these basins makes it impossible to reach the global optimum by means of a continuous gradient search along the maximum slope of the performance index, while the presence of so many attractors requires an increasing number of tests for identifying the true global optimum by means of a purely random initialization of the starting guess, as far as the global optimum can be reached only if at least one of the guesses is picked up within its basin of attraction.

As many as 500 runs were necessary for identifying the global optimum with $N = 5$. A more efficient search was thus performed by means of the MBH algorithm, briefly recalled in the Introduction. Its capability of jumping from one attractor to a neighboring one allows to reach the global optimum usually within less than a hundred runs, almost independently of N.

Results and Discussion

Thanks to the MBH approach, it was possible to find global optima for higher values of N. Both the findings of the previous subsection were confirmed for a number of rotations as high as $N = 12$, where the rotations for the optimal sequences, not reported, have equal amplitude and the axes are symmetrically distributed with respect to $\alpha = 0$, as it is clearly visible in Fig. 10, where the positions of the feasible rotation axes of the optimal sequences are reported for the same test case described in the previous subsection ($\phi = 30$ deg, $\lambda = 20$ deg).

It must also be noted that, as a matter of fact, the savings obtained in terms of total angular travel with respect to the $N = 2$ case solved analytically are significant only for a small number of rotations, say $N < 5$. As shown in Fig. 11, the total angular travel for $\phi = 30$ deg and $\lambda = 20$ deg decreases from 85 deg for $N = 2$, to 65 deg for $N = 5$, that is, almost a 20% reduction of the angular travel is obtained. For higher values of N, ϕ_{tot} is only marginally decreased: approximately 1 deg is saved increasing N to six, and the total

Table 1 Local optima for $N = 4$, $\phi = 30$ deg, $\lambda = 20$ deg

α_1	$\hat{\phi}_1$	α_2	$\hat{\phi}_2$	α_3	$\hat{\phi}_3$	α_4	$\hat{\phi}_4$	ϕ_{TOT}
−87.7420	16.4799	−29.2473	16.4799	29.2473	16.4799	87.7420	16.4799	65.9196
−87.8884	16.3637	−30.1890	16.3786	28.9649	16.6352	87.4226	16.5433	65.9208
−88.7043	15.9693	−31.3451	16.4543	27.5554	16.6842	87.1043	16.8158	65.9236
−86.3928	17.1124	−26.6862	16.4957	31.2507	16.2214	88.6603	16.0962	65.9257
−86.5812	16.1601	−31.1105	16.7257	30.2203	16.5875	88.4487	16.4658	65.9391
−90.4248	14.8766	−37.3136	16.0983	24.0849	17.4865	85.4114	17.5106	65.9719
−96.3953	13.5024	−39.2931	17.3536	22.5731	17.5268	83.7467	17.6713	66.0542
−95.4577	13.4461	−45.5756	13.6166	5.7394	17.7517	78.9007	21.5874	66.4018
−103.1684	12.7468	−45.6624	14.8485	9.4830	18.7159	78.2629	20.1083	66.4195
−96.2366	13.1213	−46.8938	13.4915	3.4783	17.7632	78.1357	22.1266	66.5027
−76.7005	22.9945	−0.6754	16.8928	44.0226	12.9318	95.7792	13.8425	66.6617
−94.7650	10.7437	−63.4233	14.8073	10.7662	21.1690	79.8513	20.1514	66.8714
−98.5443	12.4109	−51.4068	12.3846	−4.6302	18.1646	75.2716	23.9929	66.9529
−99.0646	10.1057	−66.3174	12.3044	−6.6190	20.6557	75.1127	24.2243	67.2900
−72.9824	24.5584	−52.7776	3.6479	19.6894	20.7801	86.3767	19.5879	68.5743
−84.1099	21.4047	−51.8774	0.8030	−2.4734	23.1158	79.2141	23.2611	68.5846
−66.8554	24.0741	−25.7544	13.4799	55.8753	15.6190	90.4384	15.4422	68.6152
−161.7522	0.0315	−80.8682	22.9203	0.0184	22.9197	80.8986	22.9184	68.7899
113.0134	0.0211	−80.7667	23.0157	0.2579	22.9143	81.0592	22.8762	68.8274
98.1426	0.1310	−85.5948	21.1024	−7.6620	23.3972	77.3863	24.5205	69.1511
−94.1205	20.0707	12.8028	0.0858	−8.2365	24.8910	73.6511	24.2524	69.2998
−87.0443	23.4397	12.7984	28.6330	77.6536	10.3160	100.8840	7.0528	69.4415
−80.0269	26.8387	23.4795	24.8341	57.5692	8.3913	101.0479	9.6399	69.7040
−62.4607	31.7334	38.4481	26.5543	111.5788	10.6626	121.9068	2.7188	71.6691
−141.7287	3.2774	−109.8584	16.8409	−12.1756	25.6567	59.4452	25.9652	71.7402
−55.8976	34.4344	44.9548	24.4160	114.0574	10.3926	130.1415	3.4530	72.6960

angular travel asymptotically approaches a value around 63 deg for higher values of N.

These results demonstrate that an MBH optimization approach can efficiently tackle the maneuver planning problem, for a sequence of N rotations, where N can become quite large. Nonetheless, such an increase on N is not necessary and a number of rotations between four and seven is usually sufficient for obtaining most of the savings with respect to the two-step maneuver. Higher values of N are not justified because the additional computational cost and major difficulties in the convergence are not compensated by the almost irrelevant reduction of the angular travel required by the maneuver. By formulating the optimization problem in the proposed unconstrained form, for such a small number of rotations in the sequence, convergence of the MBH method is fast, thus providing an efficient tool for maneuver planning, when a limited computation power is available.

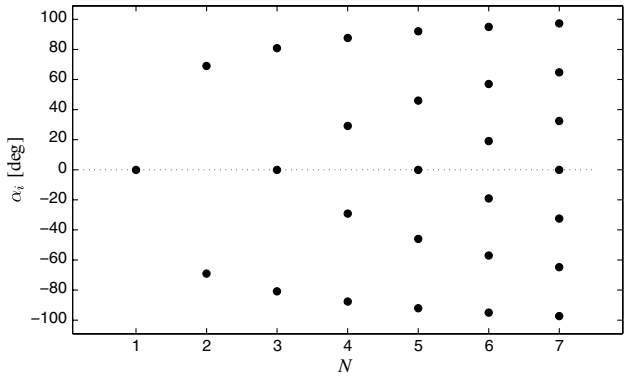

Fig. 10 Distribution of feasible rotation axes on Γ for increasing values of N ($\phi = 30$ deg, $\lambda = 20$ deg).

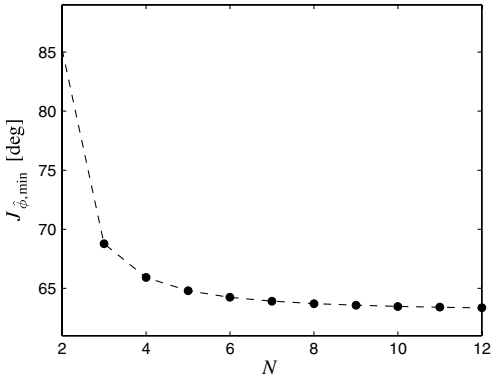

Fig. 11 Minimum total angular travel for increasing values of N ($\phi = 30$ deg, $\lambda = 20$ deg).

Conclusions

A unified geometric framework for attitude maneuver planning of underactuated spacecraft was derived, when admissible rotation axes are constrained on a plane perpendicular to the axis along which no control torque is available. A sequence of two admissible rotations, allowing a body-fixed frame to reach an arbitrary attitude in space, was analytically obtained when the constraint on admissible rotations is defined in either the body or the fixed frame. The resulting two-step maneuver was identified by means of two couples of parameters representing the position of the admissible rotations eigenaxes and amplitude of the rotations, respectively. The optimal values of such parameters resulting in the total minimum angular travel were also derived.

The general problem for the exact pointing by means of an arbitrary number N of feasible rotations was then considered by means of a numerical optimization technique for an unconstrained formulation of the problem. A MS MBH algorithm was employed in order to pursue the global minimum in the presence of several basins of attractions for local minima. Thanks to this technique, it was possible to analyze situations with N as high as 12. Global minima for each sequence are obtained for rotations of equal amplitude, with admissible rotation axes distributed symmetrically with respect to the initial position of the projection of the desired rotation eigenaxis on the plane of admissible axes. The total minimum angular travel is reduced by increasing the number of rotations, but the gain becomes less significant in most cases for values of N greater than seven.

References

[1] Psiaki, M. L., "Magnetic Torquer Attitude Control via Asymptotic Periodic Linear Quadratic Regulation," *Journal of Guidance, Control,*

and Dynamics, Vol. 24, No. 2, 2001, pp. 386–394.
doi:10.2514/2.4723

[2] Bullo, F., and Lewis, A. D., *Geometric Control of Mechanical Systems*, Springer, New York, 2005, Chap. 13.

[3] Byrnes, C. A., and Isidori, A., "On the Attitude Stabilization of a Rigid Spacecraft," *Automatica*, Vol. 27, No. 1, 1991, pp. 87–95.
doi:10.1016/0005-1098(91)90008-P

[4] Ayels, D., and Szafranski, M., "Comments on the Stabilizability of the Angular Velocity of a Rigid Body," *Systems and Control Letters*, Vol. 10, No. 1, 1988, pp. 35–39.
doi:10.1016/0167-6911(88)90037-0

[5] Sontag, E., and Sussmann, H., "Further Comments on the Stabilizability of the Angular Velocity of a Rigid Body," *Systems and Control Letters*, Vol. 12, No. 3, 1989, pp. 213–217.
doi:10.1016/0167-6911(89)90052-2

[6] Andriano, V., "Global Feedback Stabilization of the Angular Velocity of a Symmetric Rigid Body," *Systems and Control Letters*, Vol. 20, No. 5, 1993, pp. 361–364.
doi:10.1016/0167-6911(93)90014-W

[7] Morin, P., "Robust Stabilisation of the Angular Velocity of a Rigid Body with Two Controls," *European Journal of Control*, Vol. 2, No. 1, 1996, pp. 51–56.

[8] Tsiotras, P., and Schleicher, A., "Detumbling and Partial Attitude Stabilization of a Rigid Spacecraft Under Actuator Failure," AIAA Guidance, Navigation, and Control Conference, AIAA Paper 2000-4044, Denver, CO, 14–17 Aug. 2000.

[9] Krishnan, H., and McClamroch, H., "Attitude Stabilization of a Rigid Spacecraft Using Two Control Torques: a Nonlinear Control Approach Based on the Spacecraft Attitude Dynamics," *Automatica*, Vol. 30, No. 6, 1994, pp. 1023–1027.
doi:10.1016/0005-1098(94)90196-1

[10] Tsiotras, P., Corless, M., and Longuski, M., "A Novel Approach to the Attitude Control of Axisymmetric Spacecraft," *Automatica*, Vol. 31, No. 8, 1995, pp. 1099–1112.
doi:10.1016/0005-1098(95)00010-T

[11] Coron, J. M., and Kerai, E. L., "Explicit Feedback Stabilizing the Attitude of a Rigid Spacecraft with Two Control Torques," *Automatica*, Vol. 32, No. 5, 1996, pp. 669–677.
doi:10.1016/0005-1098(95)00194-8

[12] Morin, P., and Samson, C., "Time-Varying Exponential Stabilization of a Rigid Spacecraft with Two Control Torques," *IEEE Transactions on Automatic Control*, Vol. 42, No. 4, 1997, pp. 528–534.
doi:10.1109/9.566663

[13] Spindler, K., "Attitude Control of Underactuated Spacecraft," *European Journal of Control*, Vol. 6, No. 3, 2000, pp. 229–242.

[14] Tsiotras, P., and Luo, J., "Stabilization and Tracking of Underactuated Axisymmetric Spacecraft with Bounded Inputs," *Automatica*, Vol. 36, No. 8, 2000, pp. 1153–1169.
doi:10.1016/S0005-1098(00)00025-X

[15] Tsiotras, P., and Doumtchenko, V., "Control of Spacecraft Subject to Actuator Failures: State-of-the-Art and Open Problems," *Journal of the Astronautical Sciences*, Vol. 48, Nos. 2–3, 2000, pp. 337–358.

[16] Krishnan, H., McClamroch, N., and Reyhanoglu, M., "Attitude Stabilization of a Rigid Spacecraft Using Two Momentum Wheel Actuators," *Journal of Guidance, Control, and Dynamics*, Vol. 18, No. 2, 1995, pp. 256–263.
doi:10.2514/3.21378

[17] Kim, S., and Kim, Y., "Spin-Axis Stabilization of a Rigid Spacecraft Using Two Reaction Wheels," *Journal of Guidance, Control, and Dynamics*, Vol. 24, No. 5, 2001, pp. 1046–1049.
doi:10.2514/2.4818

[18] Vadali, R. S., and Junkins, L. J., "Spacecraft Large Angle Rotational Maneuvers with Optimal Momentum Transfer," *Journal of the Astronautical Sciences*, Vol. 31, No. 2, 1983, pp. 217–235.

[19] Hall, C., "Momentum Transfer in Two-Rotor Gyrostats," *Journal of Guidance, Control, and Dynamics*, Vol. 19, No. 5, 1996, pp. 1157–1161.
doi:10.2514/3.21758

[20] Bang, H., Myung, J., and Tahk, M., "Nonlinear Momentum Transfer Control of Spacecraft by Feedback Linearization," *Journal of Spacecraft and Rockets*, Vol. 39, No. 6, 2002, pp. 866–873.
doi:10.2514/2.3909

[21] Sidi, M. J., *Spacecraft Dynamics and Control: A Practical Engineering Approach*, Cambridge Univ. Press, Cambridge, England, U.K., 1997, App. C.

[22] Wisniewski, R., "Linear Time Varying Approach to Satellite Attitude Control Using Only Electromagnetic Actuation," AIAA Guidance, Navigation, and Control Conference, AIAA Paper 97-3479, Monterey, CA, 5–8 Aug. 2002.

[23] Wang, P., and Shtessel, Y. B., "Satellite Attitude Control Using only Magnetorquers," *Proceedings of the American Control Conference*, 1998, pp. 222–226.

[24] Lovera, M., and Astolfi, A., "Spacecraft Attitude Control Using Magnetic Actuators," *Automatica*, Vol. 40, No. 8, 2004, pp. 1405–1414.
doi:10.1016/j.automatica.2004.02.022

[25] Casagrande, D., Astolfi, A., and Parisini, T., "Global Asymptotic Stabilization of the Attitude and the Angular Rates of an Underactuated Non-Symmetric Rigid Body," *Automatica*, Vol. 44, No. 7, 2008, pp. 1781–1789.
doi:10.1016/j.automatica.2007.11.022

[26] Wie, B., *Space Vehicle Dynamics and Control*, AIAA, Reston, VA, 1998, Chap. 7.

[27] Giulietti, F., and Tortora, P., "Optimal Rotation Angle About a Nonnominal Euler Axis," *Journal of Guidance, Control, and Dynamics*, Vol. 30, No. 5, Sept. 2007, pp. 1561–1563.
doi:10.2514/1.31547

[28] Avanzini, G., and Giulietti, F., "Constrained Slews for Single Axis Pointing," *Journal of Guidance, Control, and Dynamics*, Vol. 31, No. 6, 2008, pp. 1813–1816.
doi:10.2514/1.38291

[29] Carpenter, J. R., Leitner, J. A., Folta, D. C., and Burns, R. D., "Benchmark Problems for Spacecraft Formation Flying Missions," AIAA Guidance, Navigation, and Control Conference, AIAA Paper 2003-5364, Austin, TX, 11–14 Aug. 2003.

[30] Wales, D. J., and Doye, J. P. K., "Global Optimization by Basin-Hopping and the Lowest Energy Structures of Lennard–Jones Clusters Containing up to 110 Atoms," *Journal of Physical Chemistry A*, Vol. 101, No. 28, 1997, pp. 5111–5116.
doi:10.1021/jp970984n

[31] Leary, R. H., "Global Optimization on Funneling Landscapes," *Journal of Global Optimization*, Vol. 18, No. 4, 2000, pp. 367–383.
doi:10.1023/A:1026500301312

[32] Addis, B., Locatelli, M., and Schoen, F., "Local Optimal Smoothing for Global Optimization," *Optimization Methods and Software*, Vol. 20, Nos. 4–5, 2005, pp. 417–437.
doi:10.1080/10556780500140029

[33] Locatelli, M., "On the Multilevel Structure of Global Optimization Problems," *Computational Optimization and Applications*, Vol. 30, No. 1, 2005, pp. 5–22.
doi:10.1007/s10589-005-4561-y

[34] Vasile, M., Minisci, E., and Locatelli, M., "On Testing Global Optimization Algorithms for Space Trajectory Design," AIAA/American Astronomical Society Astrodynamic Specialists Conference, AIAA Paper 2008-6277, Honolulu, HI, 18–21 Aug. 2008.